

AN INTEGRATED MICRO-OPTICAL SYSTEM FOR LASER-TO-FIBER ACTIVE ALIGNMENT

Koji Ishikawa, Jianglong Zhang, Adisorn Tuantranont, Victor M. Bright, and Yung-Cheng Lee

NSF Center for Advanced Manufacturing and Packaging of Microwave, Optical and Digital Electronics
University of Colorado at Boulder, CO 80309-0427, USA.

Abstract: We report a new micro-optical system for laser-to-fiber active alignment. An integrated microsystem platform, which has a thermally-actuated micromirror, a silicon etched v-groove and flip-chip bonding pads, is successfully fabricated and actuated for beam adjustment from a vertical-cavity surface-emitting laser (VCSEL) to a fiber. The micromirror has 4.0 degree maximum beam steering angle with the resolution of 0.08 degree/mA. With the steering angle reaching 2.5 degrees, the coupling efficiency improves to 80 % from 9% initial efficiency.

I. INTRODUCTION

A laser-to-fiber coupling module is one of the most important and basic elements in optical fiber networks. Currently laser-to-fiber couplings are widely used to transmit data signals in optical communications. Although existing commercial laser-to-fiber couplings have high coupling efficiency, they commonly need time-consuming processes and expensive external robotic control for adjusting alignment. Different alignment concepts have been recently proposed and used as inexpensive optoelectronics packaging technologies. They typically use etched v-grooves or solder self-alignment function to achieve high coupling efficiency [1-2]. However, the accuracy of those passive alignment methods cannot be improved better than $\pm 2 \mu\text{m}$. This accuracy is insufficient for high performance optical communications.

MEMS (Micro-Electro-Mechanical Systems) technology is an attractive way to direct and adjust a laser beam into an optical fiber, and assemble laser-to-fiber coupling modules. One attempt at a laser-to-fiber coupling module using MEMS has been demonstrated [3]. 40% coupling efficiency was achieved from a laser to a single-mode fiber and the results showed that MEMS have high potential for application in a laser-to-fiber coupling system. However, since their method still needs external alignment of each component, it cannot be replaced with mass productive fabrication and packaging processes. Also the components configuration and the large actuator mechanism negate the inherent size advantage of MEMS.

We have designed and fabricated a new integrated microsystem for laser-to-fiber alignment. Fig. 1 shows a

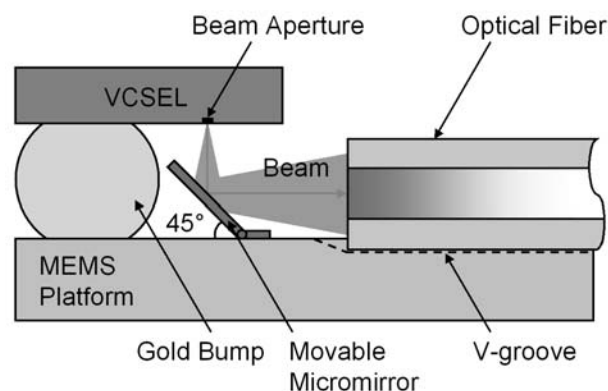


Figure 1. A cross-sectional schematic view of laser-to-fiber coupling concept.

schematic cross-sectional view of our laser-to-fiber alignment concept. The compact module consists of three parts: a VCSEL (Vertical-Cavity Surface-Emitting Laser), a thermally-actuated micromirror, and an optical fiber. The VCSEL is assembled facedown above the micromirror, and the fiber is mounted on a v-groove etched in the MEMS platform. The beam from the VCSEL is reflected and steered by the micromirror to couple to the fiber. The module is designed and packaged with mass production in mind, all of the processes used in the fabrication of this laser-to-fiber coupling are compatible with existing MEMS technologies and optoelectronics packaging manufacturing infrastructures such as flip-chip bonding, anisotropic silicon bulk etching and a solder self-assembly process [4]. Since all functions are integrated in the MEMS platform, there is no need to use extra dies or components. Thus this well-organized micro-optical system can be used to existing commercial VCSEL-to-fiber modules that are based on the packaging technique of light emitting from a VCSEL and coupled to a fiber through a fixed 45° reflector [5-6]. In this paper the details of the design, fabrication process and testing of the micro-optical system for active alignment are described.

II. DESIGN AND FABRICATION

The MEMS platform is designed and fabricated using the MUMPs (Multi-User MEMS Processes) foundry. The MUMPs process provides two structural polysilicon layers and a metal layer. Fig. 2 shows the

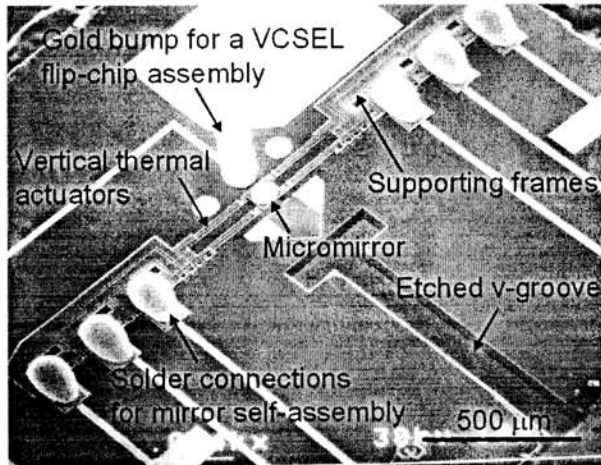


Figure 2. A top-view micrograph of the pre-assembled MEMS platform.

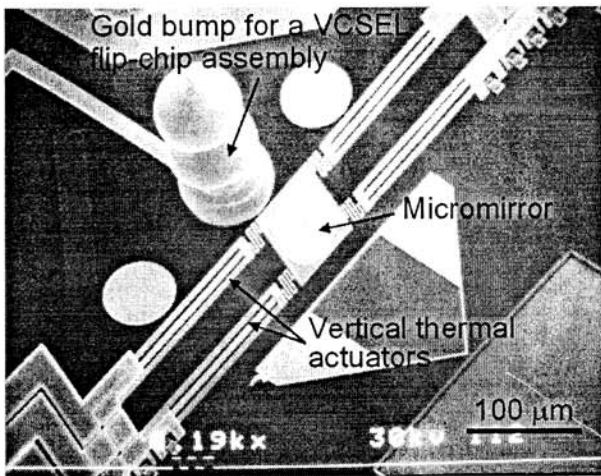


Figure 3. A close-up view of the micromirror assembled to 45° relative to the substrate.

pre-assembled MEMS platform before removing sacrificial layers. Also Fig. 3 shows a close-up view of the movable micromirror after assembly. Before removal of the sacrificial silicon dioxide layers, a v-groove is anisotropically etched to a 15 μm depth using an EDP (Ethylenediamine Pyrocatechol) solution. Then the solder connections are preformed using 4-mil diameter Sn63Pb37 solder balls. The gold bump for the VCSEL flip-chip is fabricated using a wire bonding machine. The movable micromirror structure consists of two stacked polysilicon (poly-1 and poly-2) layers with a metal layer. The square mirror plate has an area of 80 $\mu\text{m} \times 80 \mu\text{m}$ with a 72 μm diameter metal layer. The micromirror is suspended by four vertical thermal actuators, and the actuators are connected to the supporting frames. These structures are lifted up using a solder self-assembly process, which fixes them at 45°

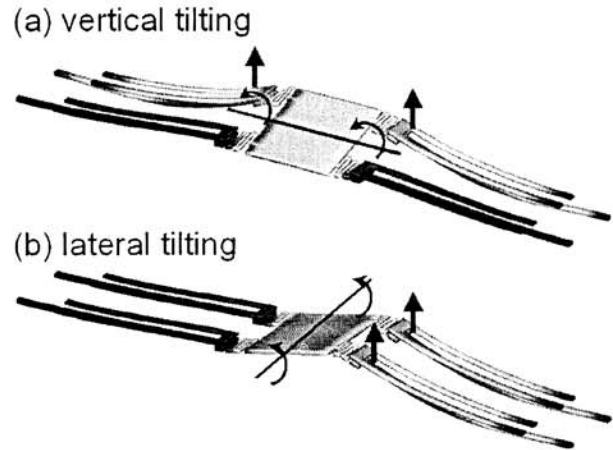


Figure 4. Schematic views of two-dimensional mirror motions (a) vertical tilting (b) lateral tilting.

with mechanical locking mechanisms. Electrical power for actuators comes from the substrate through the solder connections.

As shown in Fig. 1, the butt-coupling concept is used to demonstrate the laser-to-fiber coupling. Therefore the 45° micromirror only needs two degrees of freedom to steer the beam from the laser into the fiber. The combination of the motions of four vertical thermal actuators provides the two dimensional mirror motions [7]. Applying current, a single vertical thermal actuator moves up-and-down due to thermal expansion difference between a center poly-1 cantilever with 200 μm -length (hot arm) and side poly-2 cantilevers with 160 μm -length (cold arms). By controlling each actuator, the micromirror can be steered. When driving only two upper actuators, the micromirror rotates vertically as shown in Fig.4 (a). Using the same principle, the micromirror is steered laterally by driving the two right side actuators as shown in Fig. 4 (b). The maximum beam steering angle of 4.0 degrees can be respectively achieved in both vertical and lateral directions. Also when only one actuator is moved, the micromirror can be tilted diagonally. The combination of thermal actuator motions provides a 15 μm -radius steerable area at the tip of the optical fiber placed at a 300 μm distance from the micromirror. Since $\pm 10 \mu\text{m}$ alignment accuracy can be obtained after all assemblies, this mirror controllability is enough to adjust the beam.

Fig. 5 shows the relationship between actuators driving current and the beam steering angle. The micromirror displays fine controllability with an actuation rate of 0.08 degree/mA. Thus precise tuning is possible to obtain high coupling efficiency. Fig. 6 shows the completely assembled 2 mm \times 2 mm MEMS platform with the flip-chipped VCSEL. After lifting up the mirror structure, the VCSEL laser chip (size: 500

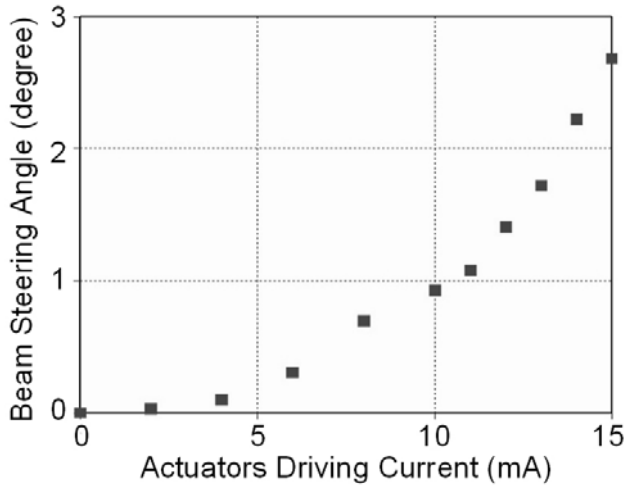


Figure 5. Beam steering angle as a function of actuators driving current.

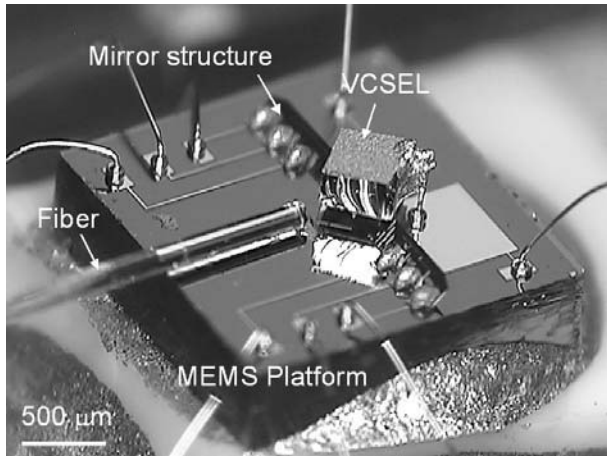


Figure 6. A photograph of the completed micro-optical system for laser-to-fiber coupling.

$\mu\text{m} \times 500 \mu\text{m} \times t250 \mu\text{m}$) is flip-chipped facedown, and the backside electrode of the VCSEL is connected with the substrate using conductive epoxy. The gold bonding bump also functions as an electrical connection with the substrate. The final gap between the VCSEL and the MEMS platform after the flip-chip process is $65 \mu\text{m}$. Last of all, the optical fiber is mounted and glued onto the v-groove. The final device size is quite compact, and it is reasonable to say that the packaging approach has scalability to VCSEL-to-fiber coupling arrays

To fabricate the laser-to-fiber coupling prototype, an existing VCSEL chip is used. Therefore the design flexibility of the MEMS platform structure is restricted by the VCSEL configuration such as the chip size, the electrode position and the beam aperture position. However, our laser-to-fiber coupling concept will be more manufacturable if a suitable VCSEL chip is used.

For example, if all electrodes are larger and on the one side, the VCSEL bonding process becomes much simpler and the design flexibility of micromirror is also expanded.

III. TESTING

The coupling efficiency from the VCSEL to the multi-mode fiber is measured. The coupling efficiency is defined as the ratio between the VCSEL output power and the optical intensity obtained from the fiber end through the micro-optical system. Optical intensity is measured by using an optical power meter. The VCSEL output power is $375 \mu\text{W}$ with an 850 nm wavelength, and a $100 \mu\text{m}$ core-diameter multi-mode fiber is used as a fiber coupling. The total optical path length from the VCSEL to the fiber end is $500 \mu\text{m}$.

Fig. 7 shows the coupling efficiency as a function of the beam steering angle. Moving two side actuators and laterally steering from left to right, the VCSEL-to-multi-mode fiber coupling efficiency can be changed and a maximum coupling efficiency of 80 % is achieved. Fig. 8 shows the ability of the micromirror to compensate for an optical fiber that is offset $25 \mu\text{m}$ from the center of the v-groove. A schematic illustration of this arrangement is shown in Fig. 9. Although the initial coupling efficiency is 9 %, the coupling efficiency is significantly improved according by the change in beam steering angle, and a maximum coupling efficiency of more than 80% is obtained. The result shows that the micromirror can compensate a fiber position misalignment within $25 \mu\text{m}$. In the integrated micro-optical system, total positioning misalignment during fabrication is predicted as $\pm 10 \mu\text{m}$. Thus, the results of the beam steering performance tests show that the MEMS platform does not need external alignment or manipulation to assemble lasers and fibers.

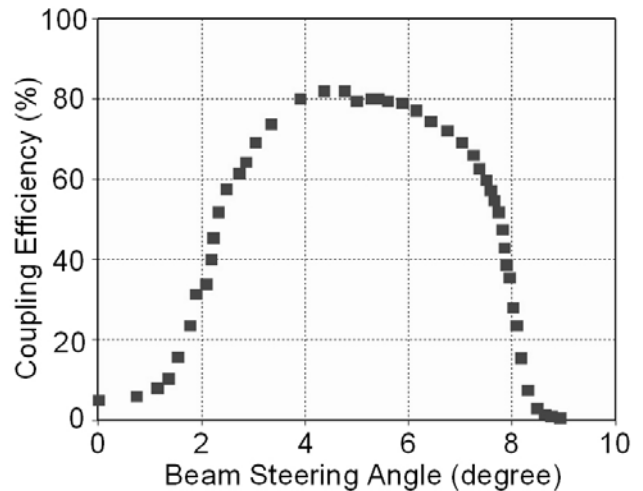


Figure 7. Coupling efficiency as a function of beam steering angle (lateral mirror tilt).

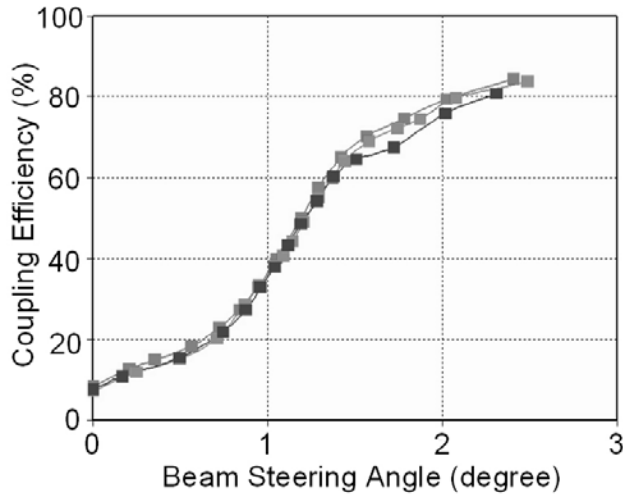


Figure 8. Coupling efficiency change versus the beam steering angle for a fiber shifted 25 μm .

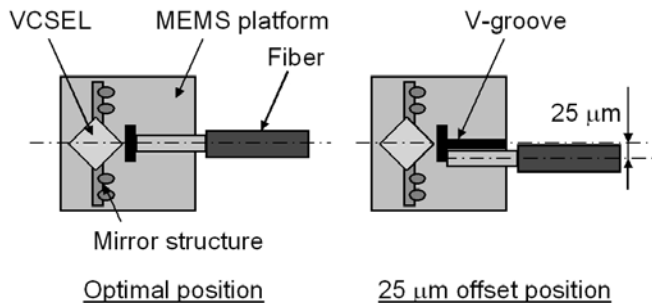


Figure 9. A schematic illustration of the coupling efficiency measurement set-up.

Also good alignment repeatability appears in Fig. 8. The same hysteresis are obtained in three separate measurements.

IV. CONCLUSION

A new micro-optical system for laser-to-fiber active alignment is successfully demonstrated using MEMS and optoelectronics packaging technologies. The prototype shows not only packageability but also high performance in coupling a beam to couple to an optical fiber. It is concluded that the simple alignment concept can be applied to current coupling modules without extra cost, and enhances coupling efficiency from a laser to a fiber.

The primary advantages of the new MEMS-based laser-to-fiber coupling approach are:

- 1) Fully automated active alignment can be provided without using external expensive precision robotic control.

- 2) Batch assembly with hundreds of MEMS-actuated laser-to-fiber alignments are possible due to mass productive module configuration.
- 3) The module assembling processes are compatible with existing passive and high-speed placement of the VCSEL and the fiber onto the platform.
- 4) The compact, simple module concept has scalability for laser-to-fiber arrays.

However, in laser-to-fiber coupling products, the micromirror position has to be permanently fixed. In this paper, the prototype does not include structures to fix the mirror position, and a method of holding the position has not been reported. In the future, the details of the fixing mechanism for a second generation device will be reported.

V. ACKNOWLEDGEMENT

This research and development was partially funded by DARPA: FAME Grant # F33615-98-C-5429. The authors would like to thank Christine Mollenkopf of Cielo Communications. Also we would like to thank Wenge Zhang, Kevin Harsh and Brian Schaible for their valuable discussions during this research. The authors also wish to thank NHK Spring Co., Ltd. for their support.

VI. REFERENCES

- [1] M. C. Cohen, M. F. Cina, E. Bassous, M. M. Opyrsko, J. L. Speidell, F. J. Frank, and M. J. DeFranza, *IEEE Trans. on Component. Hybrid. and Manufact. Technol.*, vol. 15, no. 6, pp. 944-954, Dec. 1992.
- [2] R. G. Nakagawa, K. Miura, S. Sasaki, and M. Yano, *J. of Lightwave Technol.*, vol. 14, no. 6, pp. 1519-1523, June 1996.
- [3] M. J. Daneman, O. Solgaard, N. C. Tien, K. Y. Lau, and R. S. Muller, *IEEE Photon. Technol. Lett.*, vol. 8, no. 3, pp. 396-398, January 1996.
- [4] K. F. Harsh, V. M. Bright, and Y. C. Lee, *Sensors and Actuators, A: Physical*, **77**, 1999, pp. 237-244.
- [5] H. Karstensen, *Proc. IEEE LEOS*, pp. 226-227, 1995.
- [6] L. Buckman, A. Yuen, K. Giboney, P. Rosenberg, J. Straznicky, K. Wu, and D. Dolfi, *Proc. Hot Interconnects VI*, pp. 137-143, Stanford, CA, Aug. 1998.
- [7] K. F. Harsh, W. Zhang, V. M. Bright and Y. C. Lee, *MEMS '99*, pp. 273-278.